

# Stability of Symmetric and Asymmetric Vortices over Slender Conical Wing-Body Combinations

Jinsheng Cai\*

National University of Singapore, Singapore 117508, Republic of Singapore  
and

Shijun Luo† and Feng Liu‡

University of California, Irvine, Irvine, California 92697-3975

**Theoretical analyses of the stability of symmetric and asymmetric vortex pairs over slender conical wing-body combinations consisting of a slender circular or elliptic cone and a flat-plate delta wing under small perturbations in an inviscid incompressible steady flow at high angles of attack with or without sideslip are presented. The three-dimensional flow problem is reduced to a problem in two dimensions, for which a general stability condition for vortex pairs can be applied. The stationary positions of symmetric and asymmetric vortex pairs and their stabilities are examined for various geometric configurations, angles of attack, and sideslip. Results of the analyses are compared with available experimental data and used to help gain insight into the flow behavior.**

## Nomenclature

$b$	=	$y$ semiaxis of elliptic cross section of body
$c$	=	$x$ semiaxis of elliptic cross section of body
$D$	=	divergence of vortex velocity in crossflow plane
$D_0$	=	divergence of vortex velocity at stationary point
$i$	=	$\sqrt{-1}$
$J$	=	Jacobian of vortex velocity in crossflow plane
$J_0$	=	Jacobian of vortex velocity at stationary point
$j$	=	$1, 2, \dots, N$
$K$	=	Sychev similarity parameter, $\tan \alpha / \tan \epsilon$
$K_S$	=	sideslip similarity parameter, $\tan \beta / \sin \alpha$
$N$	=	number of point sources
$Q_j$	=	strength of point source at $Z_j$
$\mathbf{q}$	=	vortex-velocity vector in crossflow plane
$r$	=	radius of conformal-mapping circle in plane $\zeta$
$s$	=	semispan of flat-plate delta wing
$U_n$	=	$U_x + iU_y$
$U_x$	=	$x$ component of freestream velocity, $U_\infty \cos \beta \sin \alpha$
$U_y$	=	$y$ component of freestream velocity, $U_\infty \sin \beta$
$U_z$	=	$z$ component of freestream velocity, $U_\infty \cos \beta \cos \alpha$
$U_\infty$	=	freestream velocity
$u, v$	=	velocity components in crossflow plane
$x, y, z$	=	rectangular body coordinate axes (Fig. 1)
$Z$	=	$x + iy$
$\alpha$	=	angle of attack
$\beta$	=	sideslip angle
$\Gamma$	=	vortex strength
$\gamma$	=	body-width-to-wing-span ratio, $b/s$
$\Delta x, \Delta y$	=	perturbation of vortex coordinates
$\epsilon$	=	semivertex angle of delta wing
$\zeta$	=	$\xi + i\eta$
$\kappa$	=	parameter in conformal mapping
$\lambda_1, \lambda_2$	=	two eigenvalues of vortex dynamic equations

$\tau$	=	body thickness ratio, $c/b$
$\phi, \varphi$	=	intermediate complex variables in conformal mappings

## Superscript

$\bar{()}$	=	complex conjugate of $()$
------------	---	---------------------------

## I. Introduction

IT is well recognized that the flow over pointed slender bodies becomes asymmetric at high angles of attack. The subject has been studied extensively in relation to air-vehicle aerodynamics because of interest in improving maneuverability by extending flight envelopes to high angles of attack. The subject has been reviewed by Hunt,<sup>1</sup> Ericsson and Reding,<sup>2</sup> and Champigny.<sup>3</sup> It is found by many experimental<sup>4,5</sup> and computational<sup>6-8</sup> studies that microasymmetric perturbations close to the nose tip produces a strong flow asymmetry. There seems to be little doubt that the vortex asymmetry is triggered, formed, and developed in the apex region, and the after portion of the forebody and the after cylindrical body (if any) have little effect on the asymmetry. The evolution of small flow perturbations near the apex plays an important role in determining the flow pattern over the entire body.

Because the apex portion of any slender pointed body is nearly a conical body, high angle-of-attack flow about slender conical bodies has been studied extensively. Dyer et al.<sup>9</sup> and Chin et al.<sup>10</sup> investigated the existence of stationary symmetric and asymmetric vortex flows over circular cones. Pidd and Smith<sup>11</sup> studied a spatial, or otherwise called convective, type of instability of the stationary symmetric and asymmetric vortices found by Dyer et al.<sup>9</sup> Huang and Chow<sup>12</sup> used a simplified vortex model and succeeded in showing analytically that the vortex pair over a slender flat-plate delta wing at zero sideslip can be stationary and is stable under small conical perturbations, which agreed with the experimental results of Stahl et al.<sup>13</sup>

The present authors<sup>14</sup> developed a general stability condition for vortices in a two-dimensional incompressible inviscid flowfield and a mathematical framework to reduce the problem of a three-dimensional flow over slender conical bodies at high angles of attack to the solution of a two-dimensional problem. The method was applied to analyze the absolute (temporal) stability of symmetric vortex pairs over three-dimensional slender conical bodies. The bodies considered include circular cones and highly swept flat-plate delta wings with and without vertical fins and elliptic cones of various eccentricities. Results based on the theory agreed well with known

Received 24 August 2005; revision received 28 November 2005; accepted for publication 28 November 2005. Copyright © 2006 by the authors. Published by the American Institute of Aeronautics and Astronautics, Inc., with permission. Copies of this paper may be made for personal or internal use, on condition that the copier pay the \$10.00 per-copy fee to the Copyright Clearance Center, Inc., 222 Rosewood Drive, Danvers, MA 01923; include the code 0001-1452/06 \$10.00 in correspondence with the CCC.

\*Research Scientist, Temasek Laboratories.

†Researcher, Department of Mechanical and Aerospace Engineering.

‡Professor, Department of Mechanical and Aerospace Engineering, Associate Fellow AIAA.

experimental observations. The authors further extended their previous analysis to include asymmetric vortices over slender conical bodies in Ref. 15.

Because of the undesirable effects associated with the forebody flow asymmetries, numerous means of alleviating the problem have been devised. One method makes use of nose strakes. Coe et al.<sup>16</sup> showed by wind-tunnel tests alleviating effects of horizontal strakes placed close to the apex of a slender ogive forebody and a circular cone. Champigny<sup>3</sup> showed that when a pair of narrow wings is located very far forward on the pointed nose of an ONERA-S3MA model the side forces at high angles of attack are substantially reduced. Erickson and Lorincz<sup>17</sup> showed via water-tunnel visualization that the symmetric forebody vortices developed on an F-18-type configuration at high angle of attack and zero sideslip were strongly entrained on to the wing by the powerful vortices shed from the wing leading-edge extensions. Nelson and Malcolm<sup>18</sup> investigated the surface and wake flow around a high-performance aircraft model at a 20-deg angle of attack. Moreover, forebody strakes were shown to provide high levels of yawing control at extremely high angles of attack where conventional aerodynamic controls are ineffective as shown by experimental studies (for example, see Malcolm<sup>19</sup> and Murri and Rao<sup>20</sup>).

In view of the preceding experimental studies and the importance of the related applications, we extend in this paper our previous analysis in Refs. 14 and 15 to include symmetric and asymmetric (if any) vortices over slender conical wing-body combinations. The vortex model used for wing-body combination is first described. The analytical method is briefly reviewed. The stability of stationary symmetric and asymmetric vortex flows over slender flat-plate delta wing and circular or elliptic cone combinations with and without sideslip is analyzed by the present theory. Comparisons are made with available experimental observations. The theoretical analyses help gain insight into the flow physics of the observed experimental phenomena. In addition, the analytical flow models developed in this paper can potentially serve as reduced-order models to facilitate development of active flow-control algorithms for practical three-dimensional vortex flows over wing-body combinations in the manner as demonstrated by Protas<sup>21</sup> in two dimensions.

## II. Flow Model and the Stability Analysis Method

Consider the flow past a slender conical wing-body combination at an angle of attack  $\alpha$  and sideslip angle  $\beta$  as shown in Fig. 1 with the rectilinear body coordinates  $(x, y, z)$ . The velocity of the freestream flow is  $U_\infty$ . The combination has a slender triangular flat-plate wing passing through the longitudinal axis of the body. The flow separates from the wing sharp leading edge, and the flow is assumed to be steady, inviscid, incompressible, conical, and slender. The reader is referred to Refs. 14 and 15 for details of the theoretical background and validity of the assumptions. The following subsections summarize the necessary equations for the wing-body combinations under present consideration.

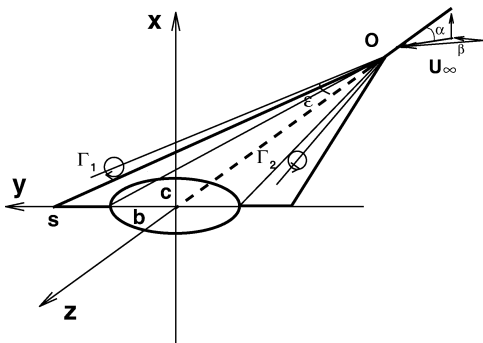


Fig. 1 Slender conical wing-body combination and separation vortices.

### A. Positions and Strengths of Stationary Vortices

The inviscid incompressible flow considered in the preceding model is irrotational except at the centers of the isolated vortices. The governing equation for the velocity potential is the three-dimensional Laplace equation with zero normal flow velocity on smooth body surfaces and Kutta conditions at sharp edges as boundary conditions. By the principle of superposition, the flow around the body can be obtained by solving the following two flow problems: 1) the flow caused by the normal components of the freestream velocity,  $U_x = U_\infty \cos \beta \sin \alpha$  and  $U_y = U_\infty \sin \beta$ ; and 2) the flow caused by the axial component of the freestream velocity,  $U_z = U_\infty \cos \beta \cos \alpha$ , both subject to the boundary conditions.

Under the assumption of conical and slender-body flow, the three-dimensional flow problem is reduced to a two-dimensional flow problem. In a conical flow the flow properties are constant along rays from the apex of the conical body. The slender-body assumption assumes that the flow varies slowly along the longitudinal body axis so that derivatives in the longitudinal direction can be neglected in the governing equation for the crossflow. The flow in each cross section at  $z$  can then be regarded as a two-dimensional flow across the local cross-sectional profile governed by the two-dimensional Laplace equation with the boundary conditions. Solution to this two-dimensional velocity field can be obtained by conformal mapping or other analytical or numerical methods. For simple profiles such as a wing-elliptic-body combination, the conformal mapping for this profile in the plane  $Z = x + iy$  to a circle of radius  $r$  in a uniform flow of velocity  $(U_x/2, U_y/2)$  in the plane  $\zeta = \xi + i\eta$  is

$$Z = \frac{1}{2}(\phi + \kappa/\phi), \quad \phi = \varphi + \sqrt{\varphi^2 + 1}, \quad \varphi = \frac{1}{2}(\zeta - r^2/\zeta)$$

where  $c = (1 + \kappa)/2$ ,  $b = (1 - \kappa)/2$ , and  $r = [bs - c\sqrt{(s^2 + 2c - 1)/(1 - 2c)}]$ . Two geometric parameters are defined, which will be referenced to extensively in the discussions: the thickness ratio of the centerbody  $\tau \equiv c/b$ , and  $\gamma \equiv b/s$ .

The complex velocity on the crossflow plane  $Oxy$  is

$$\begin{aligned} u - iv = & \left[ \frac{1}{2} \left( \overline{U_n} - \frac{U_n r^2}{\zeta^2} \right) + \frac{i\Gamma_1}{2\pi} \left( \frac{1}{\zeta - \zeta_1} - \frac{1}{\zeta - r^2/\zeta_1} \right) \right. \\ & \left. - \frac{i\Gamma_2}{2\pi} \left( \frac{1}{\zeta - \zeta_2} - \frac{1}{\zeta - r^2/\zeta_2} \right) \right] \left( \frac{d\zeta}{dZ} \right) \\ & - \frac{U_x \bar{Z}}{sK} + \frac{1}{2\pi} \sum_{j=1}^N \frac{Q_j}{Z - Z_j} \end{aligned} \quad (1)$$

where the overbar denotes complex conjugate;  $U_n = U_x(1 + iK_S)$ ;  $K_S = \tan \beta / \sin \alpha$  is the sideslip similarity parameter;  $K = \tan \alpha / \tan \epsilon$  is the Sychev similarity parameter<sup>22</sup>;  $\zeta_1$  and  $\zeta_2$ , and  $\Gamma_1$  and  $\Gamma_2$  are the positions and strengths of the vortex 1 and vortex 2, respectively; and  $Q_j$  is the strength of the point sources at  $Z_j$  and  $Q_j (j = 1, 2, \dots, N)$  are to be determined by  $N$  simultaneous equations of the boundary condition on the body contour.

The complex velocity at the vortex point  $Z_1$  (or  $\zeta_1$ ) is obtained by a limiting process<sup>23</sup>:

$$\begin{aligned} u_1 - iv_1 = & \left[ \frac{1}{2} \left( \overline{U_n} - \frac{U_n r^2}{\zeta_1^2} \right) + \frac{i\Gamma_1}{2\pi} \left( -\frac{1}{\zeta_1 - r^2/\zeta_1} \right) \right. \\ & \left. - \frac{i\Gamma_2}{2\pi} \left( \frac{1}{\zeta_1 - \zeta_2} - \frac{1}{\zeta_1 - r^2/\zeta_2} \right) \right] \left( \frac{d\zeta}{dZ} \right)_1 \\ & - \frac{i\Gamma_1}{4\pi} \left( \frac{d^2 Z}{d\zeta^2} \right)_1 \left( \frac{d\zeta}{dZ} \right)_1^2 - \frac{U_x \bar{Z}_1}{sK} + \frac{1}{2\pi} \sum_{j=1}^N \frac{Q_j}{Z_1 - Z_j} \end{aligned} \quad (2)$$

where the subscript 1 denotes the values at  $Z = Z_1$  (or  $\zeta = \zeta_1$ ). A similar expression is obtained for the complex velocity  $u_2 - iv_2$  at the vortex point  $Z_2$  (or  $\zeta_2$ ).

The stationary positions  $Z_1$  (or  $\zeta_1$ ) and  $Z_2$  (or  $\zeta_2$ ) and strengths of the vortices  $\Gamma_1$  and  $\Gamma_2$  are determined by solving a set of algebraic equations. These are  $u_1 - i v_1 = 0$  and  $u_2 - i v_2 = 0$  for the vortex velocity fields and two more equations that set the flow velocities to be finite values at the sharp edges of the flat plate (Kutta condition). The four algebraic equations are linear in  $\Gamma_1$  and  $\Gamma_2$  and nonlinear in  $Z_1$  (or  $\zeta_1$ ) and  $Z_2$  (or  $\zeta_2$ ). They are solved by an iteration method. A Newton iteration for the vortex locations is constructed for  $\mathbf{F}(\mathbf{X}) = 0$ , where  $\mathbf{F} = [u_1, v_1, u_2, v_2]^T$ ,  $\mathbf{X} = [\xi_1, \eta_1, \xi_2, \eta_2]^T$ ,  $\zeta_1 = \xi_1 + i\eta_1$ , and  $\zeta_2 = \xi_2 + i\eta_2$ . Given the vortex positions  $\zeta_1$  and  $\zeta_2$ , the vortex strengths  $\Gamma_1$  and  $\Gamma_2$  can be obtained.

### B. Stability of the Stationary Vortices

When a vortex is slightly perturbed from its stationary position, the increments of its coordinates as function of time are governed by a system of linear homogeneous first-order ordinary differential equations as shown in Ref. 14. The perturbations can be decomposed into a symmetric perturbation  $Z_1 = Z_{10} + \Delta Z$ ,  $Z_2 = Z_{20} + \overline{\Delta Z}$  and an antisymmetric perturbation  $Z_1 = Z_{10} + \Delta Z$ ,  $Z_2 = Z_{20} - \overline{\Delta Z}$ , where  $\Delta Z = \Delta x + i\Delta y$ ,  $|\Delta x| \ll s$ , and  $|\Delta y| \ll s$ . The eigenvalues of the coefficient matrix in the dynamic equations are  $\lambda_1$  and  $\lambda_2$ . Define the Jacobian and divergence of the vortex velocity field  $\mathbf{q} = (u, v)$ :

$$J = \begin{pmatrix} \frac{\partial u}{\partial x} & \frac{\partial u}{\partial y} \\ \frac{\partial v}{\partial x} & \frac{\partial v}{\partial y} \end{pmatrix}, \quad D = \nabla \cdot \mathbf{q} = \frac{\partial u}{\partial x} + \frac{\partial v}{\partial y} \quad (3)$$

It can be easily shown that the eigenvalues of this problem are

$$\lambda_{1,2} = \frac{1}{2}(D_0 \pm \sqrt{D_0^2 - 4J_0}) \quad (4)$$

where the subscript 0 denotes values at  $(x_0, y_0)$ . The maximum real part of the two eigenvalues  $\lambda_1$  and  $\lambda_2$  in Eq. (4) will be plotted and used to determine stability in this paper. A positive value of this variable means instability of the vortex system. A necessary condition for a vortex configuration to persist in a real flow is that all vortices in the system be stable in response to both symmetric and antisymmetric perturbations.

The type of instability studied in the present paper is the absolute type of instability, which describes the temporal evolution of the conical symmetric or asymmetric vortices. Satisfaction of this ‘‘absolute’’ type of stability condition should be regarded as one necessary condition for any configuration of a conical symmetric or asymmetric vortex pattern to persist in a flow as was discussed in Refs. 14 and 15. The vortices considered in these analyses are assumed strictly conical. Once a stationary symmetric and asymmetric conical vortex pair is determined to be unstable, the vortices are likely nonconical, unsteady, or both.

### III. Analysis of Typical Model Configurations

To put in perspective the analytic results obtained next for the wing-body combinations, it is useful to first review the vortex flow characteristics of isolated wing and isolated body at high angles of attack obtained in the previous paper<sup>15</sup> by the present authors.

For a slender flat-plate delta wing, there exist no stationary asymmetric vortices unless there is sideslip. Both the stationary symmetric vortices at zero sideslip and the asymmetric vortices at nonzero sideslip are stable.

For a slender circular cone, both symmetric and asymmetric conical vortex pairs exist at sufficiently large angles of attack with either symmetric or asymmetric separations, but none of them are stable. This implies that a stable vortex pair, if it exists, over a slender circular cone shall be in general nonconical or curved. Keener et al.<sup>24</sup> performed experiments in the Ames 12-Foot Wind Tunnel to determine the subsonic aerodynamic characteristics of four forebodies at  $\alpha = 20\text{--}75$  deg and  $Re = 0.4\text{--}4.6 \times 10^6$  based on body diameter. The forebodies tested are a tangent ogive with fineness ratio of 5, a paraboloid with fineness ratio of 3.5, a circular cone of semivertex

angle of 10 deg, and a tangent ogive with an elliptic cross section. They found that the variation of side force is generally repeatable with increasing and decreasing angle of attack and also from test to test for all of the forebodies tested except for the cone and for the elliptic tangent ogive with a vertical major axis, for which the variation is erratic. For the circular cone, the side force changes from side to side as the angle of attack increases, which is the most erratic variation of all the forebodies tested. Moreover, the changes in side force with increasing angle of attack are accompanied by dynamic oscillations. This result indicates that neither symmetric nor asymmetric stationary conical vortex pair is stable over slender circular cone at high angles of attack, consistent with the preceding theoretical predictions. Should there exist either symmetric or asymmetric stationary stable conical vortex pair, the variation of side force with angle of attack would be steady and repeatable.

For slender elliptic cones, the behavior of the vortices is found to change gradually from that of the vortices for a circular cone to that for a flat-plate delta wing as the thickness ratio decreases from one (circular cone) to zero (flat-plate delta wing).

Reference 14 also studied the stability of the symmetric vortex pair for the combination of a flat-plate delta wing and a vertical flat-plate fin. Shanks<sup>25</sup> observed loss of symmetry of the vortex flow over a flat-plate delta wing with a slight leeward-side-fin center spline, which functioned like a short dorsal fin. The stability analysis in Ref. 14 reveals that a short dorsal fin destabilizes the vortex flow over the flat-plate delta wing, and stability is restored only when the fin exceeds a critical height. This general prediction was later verified by Meng et al.<sup>26</sup> in carefully designed wind-tunnel experiments using models with fins of heights below and above the theoretical critical height.

We proceed with presentation of new results on two representative wing-body combinations. The two geometric parameters  $\gamma$  and  $\tau$  defined in the preceding section will be frequently cited in the following discussions.

#### A. Flat-Plate Delta Wing and Circular-Cone Combinations

Consider a wing-body combination of a flat-plate delta wing and a circular-cone body with the body-width-to-wing-span ratio  $\gamma = 0.7$  at zero sideslip, that is,  $K_S = 0$ . Stationary symmetric and asymmetric vortex locations are found. Then, the stability of the stationary vortices is determined by examining the eigenvalues of the vortex system as given by Eq. (4) calculated at their stationary positions. Figure 2 shows the calculated location of stationary symmetric and asymmetric vortex pairs for a range of the Sychev similarity parameter  $K$  from 2.0 to 4.5. No stationary asymmetric vortex pair is found when  $K$  is less than 2.0. At higher  $K$ , both symmetric and asymmetric stationary vortex pairs exist. As  $K$  is increased, that is, when the flow angle of attack is increased for a given geometry, both stationary symmetric and asymmetric vortex pairs move upward and outboard. The movement of the lower vortex of the asymmetric vortex pair is much smaller, and that of the upper vortex is much greater than the movements of the symmetric vortices.

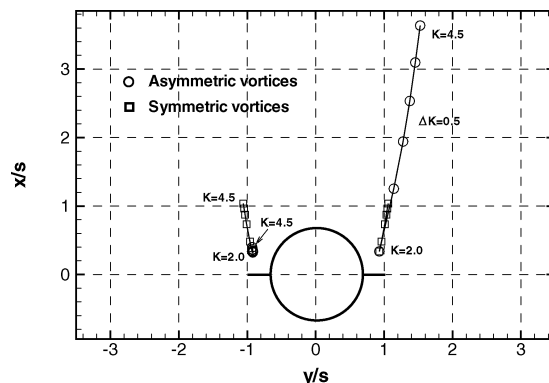


Fig. 2 Location of stationary symmetric and asymmetric vortex pairs over a wing-body combination of a flat-plate delta wing and a circular-cone body vs  $K$ ,  $\gamma = 0.7$ ,  $K_S = 0$ .

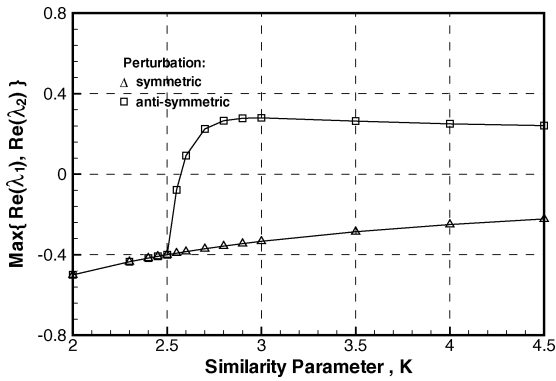


Fig. 3 Maximum real part of the eigenvalues for symmetric vortex pairs over a wing-body combination of a flat-plate delta wing and a circular-cone body vs  $K$ ,  $\gamma = 0.7$ ,  $K_S = 0$ .

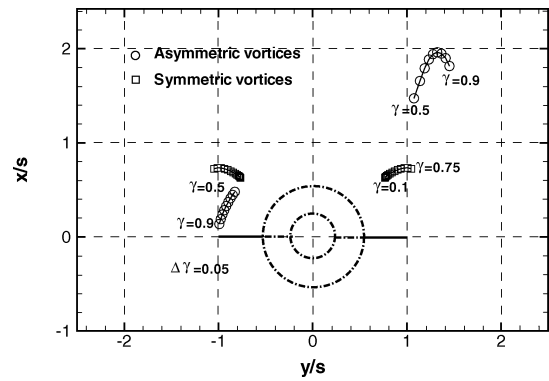


Fig. 5 Location of stationary symmetric and asymmetric vortex pairs over a wing-body combination of a flat-plate delta wing and a circular-cone body vs  $\gamma$ ,  $K = 3$ ,  $K_S = 0$ .

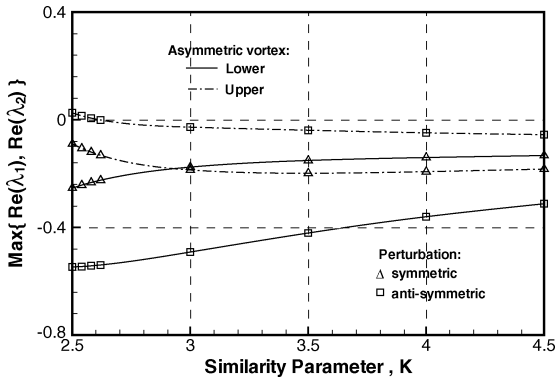


Fig. 4 Maximum real part of the eigenvalues for asymmetric vortex pairs over a wing-body combination of a flat-plate delta wing and a circular-cone body vs  $K$ ,  $\gamma = 0.7$ ,  $K_S = 0$ .

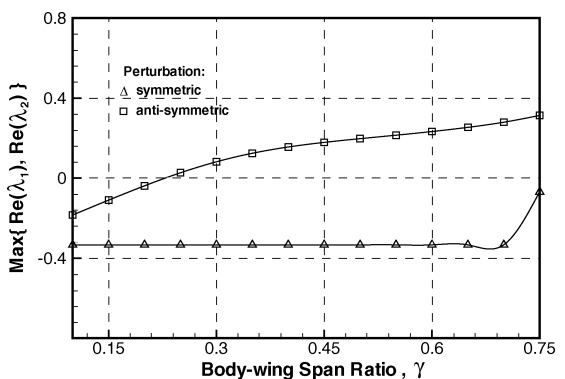


Fig. 6 Maximum real part of the eigenvalues for symmetric vortex pairs over a wing-body combination of a flat-plate delta wing and a circular-cone body vs  $\gamma$ ,  $K = 3$ ,  $K_S = 0$ .

Figure 3 shows the eigenvalues vs  $K$  for the symmetric vortex pair. (Only the maximum real part of the two eigenvalues is plotted here and in all other figures of this paper.) The symmetric vortex pair is stable for  $K \leq 2.58$  and unstable otherwise. Figure 4 shows the eigenvalues for the asymmetric vortex pair. In the calculated range of  $K$ , the lower vortex is stable, whereas the upper vortex is stable only for  $K > 2.62$ . Thus, as a whole, the asymmetric pair is unstable for  $K < 2.62$  and becomes stable when  $K$  exceeds 2.62. This indicates that an initially symmetric vortex pair at low angles of attack is likely to transit to an asymmetric pair when the angle of attack is increased beyond the critical value of  $K = 2.58 \sim 2.62$ .

The present analytical result is compared with the low-speed wind-tunnel data for a forebody strake/fuselage model made by Murri and Rao.<sup>20</sup> The tested forebody is a conical combination of a circular cone and a flat-plate delta wing of  $\gamma = 0.77$  and  $\epsilon = 12$  deg. The afterbody is a circular cylinder. The Reynolds number based on the fuselage diameter is  $1.9 \times 10^5$ . The tests showed that the onset of nonzero yawing moments occurs at about  $\alpha = 28$  deg or  $K = 2.5$ . This result agrees approximately with the preceding theoretical critical value of  $K = 2.58\text{--}2.62$  despite the slight differences between the  $\gamma$  values of the test model and the theoretical analysis. The occurrence of nonzero moments is an indication of loss of symmetry of the separation vortices over the wing-body combination.

To study the effect of the body-width-to-wing-span ratio  $\gamma$ , we examine the case with a fixed  $K = 3$  and no sideslip. Figure 5 shows the computed location of stationary symmetric and asymmetric vortex pairs for  $\gamma$  ranging from 0.1 to 0.9. No stationary asymmetric vortex pairs can be found for  $\gamma < 0.50$ . For  $\gamma \geq 0.5$  both symmetric and asymmetric vortex pairs are possible. As  $\gamma$  increases, both vortex pairs move outboard. The lower vortex of the asymmetric vortex pair goes downward toward the wing leading edge. The upper vortex goes upward first and then downward.

Figure 6 shows the eigenvalues of the symmetric vortex system vs  $\gamma$ . Increase of  $\gamma$ , that is, the size of the center circular cone relative

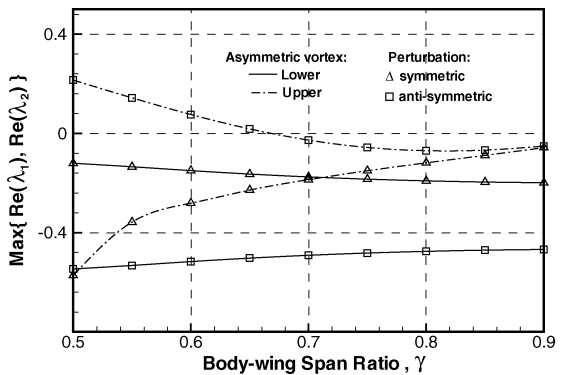


Fig. 7 Maximum real part of the eigenvalues for asymmetric vortex pairs over a wing-body combination of a flat-plate delta wing and a circular-cone body vs  $\gamma$ ,  $K = 3$ ,  $K_S = 0$ .

to the wing span destabilizes the symmetric vortices. The symmetric vortex pair becomes unstable when  $\gamma$  exceeds 0.23. However, the asymmetric vortex pair does not yet emerge until  $\gamma$  reaches 0.5. This indicates that the instability of a stationary symmetric vortex pair does not necessarily lead to the existence of a stationary asymmetric vortex pair under the same conditions. Nonconical or unsteady solutions, however, could exist.

Figure 7 shows the eigenvalues of the asymmetric vortex pair vs  $\gamma$ . The upper vortex is more unstable than the lower one under antisymmetric perturbations. (We notice from results of other cases later that this observation is true in general.) The lower vortex is stable for all  $0.5 \leq \gamma \leq 0.9$ , whereas the upper vortex is stable only for  $\gamma \geq 0.66$ . Thus, the asymmetric vortex pair as a whole is stable for  $0.66 \leq \gamma \leq 0.9$ . In the calculated range of  $\gamma$ , both the symmetric and the asymmetric vortex pairs are unstable for  $0.23 < \gamma < 0.66$ .

This implies that the vortex flow cannot be conical or steady under such conditions in this  $\gamma$  range.

Coe et al.<sup>16</sup> placed a pair of small strakes near the tip of a circular cone in their experiments to suppress vortex asymmetry. The circular cone has a semivertex angle of 8.13 deg. A pair of flat-plate strakes is placed on the nose of the cone. The planform of the small strakes is rectangular, 0.0833 cone base diameter wide  $\times$  0.583 cone base diameter long. The leading edge of the strakes is placed at 4.76% cone length behind the nose tip. The experimental Reynolds number is  $0.35 \times 10^6$ . They showed that the strakes significantly reduced the originally large asymmetric forces as the angle of attack varied from 0 to 75 deg at zero sideslip (see Fig. 24b of Ref. 16). Although no strict equivalent configuration of the present conical wing-body combination of a circular cone and a flat-plate delta wing can be made to the preceding experimental setup, an approximation is made by using a strake of conical planform whose leading edges pass through the two front corners of the rectangular strakes in the experiment on consideration that the separation vortices must start from these corner points. This leads to a semiapex angle  $\epsilon$  of 30 deg, resulting in a  $\gamma$  of close to 0.25. Figure 6 shows a critical  $\gamma$  value of about 0.25 for the given  $K$  value of 3.0. In other words, it indicates that the symmetric vortex pair over a model with  $\gamma = 0.25$  is stable for  $K$  up to 3, which converts to  $\alpha = 60$  deg for the experimental model. The theoretical analysis is consistent with the experimental observations. By placing a pair of horizontal strakes near a pointed body nose, the original separation lines move from the smooth body surface to the sharp edges of the strakes. If the strakes are wide enough, the vortex-flow characteristics change from those for a pointed body of revolution to those for a sharp-edge delta wing, for which we know that the symmetric vortex pair is stable.

It is known that placing a triangular flat-plate fin of enough height near the tip of pointed body in the leeward incidence plane can also reduce the vortex asymmetry at high angles of attack as shown by the experiments of Asghar et al.<sup>27</sup> and Ng<sup>28</sup> and confirmed with the analytical results of the present authors in Ref. 14. The vertical fins work with a different mechanism of suppressing the vortex asymmetry from that of the horizontal strakes. The vertical fins suppress the vortex asymmetry by hindering the interaction between the symmetric vortex pair at high angles of attack, while the horizontal strakes suppress the vortex asymmetry by forcing the separation line to the leading edge of the strakes and stretching the two symmetric concentrated vortices away from each other to reduce the interaction between the two vortices.

Finally, we study the situation with sideslip for a wing-body combination with  $\gamma = 0.3$  and  $K = 3$ . Figure 8 shows the possible stationary asymmetric vortex pairs for the sideslip similarity parameter  $K_S$  in the range from 0.0 to 0.6. There are no stationary asymmetric vortex pairs at zero sideslip for this set of  $\gamma$  and  $K$  values. When the sideslip similarity parameter  $K_S$  increases from zero, the windward (right-hand side) vortex of the initially symmetric vortex pair goes slightly inboard and downward, and the leeward (left-hand side) vortex stretches significantly outboard and upward. Figure 9 shows the eigenvalues vs the sideslip similarity parameter  $K_S$ . The

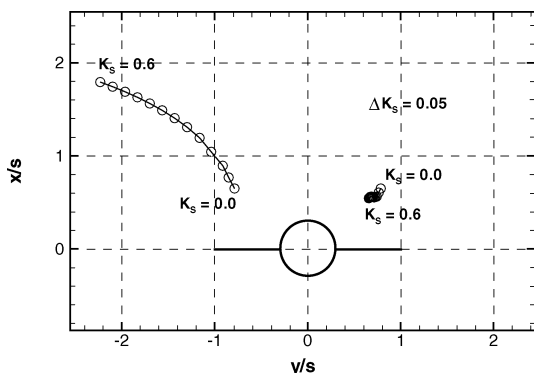


**Fig. 8** Location of stationary vortex pairs over a wing-body combination of a flat-plate delta wing and a circular-cone body vs  $K_S$ ,  $\gamma = 0.3$ ,  $K = 3$ .

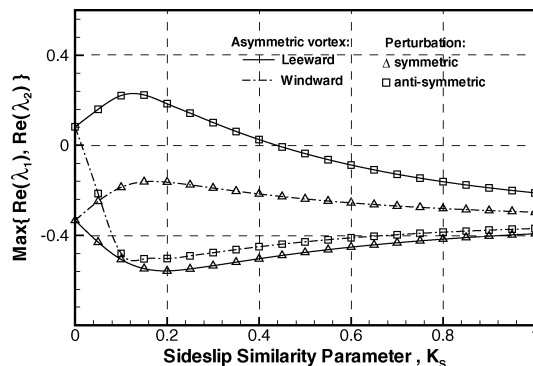


**Fig. 9** Maximum real part of the eigenvalues for asymmetric vortex pairs over a wing-body combination of a flat-plate delta wing and a circular-cone body vs  $K_S$ ,  $\gamma = 0.3$ ,  $K = 3$ .

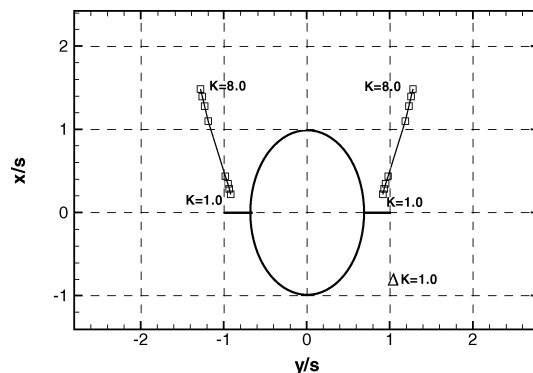


**Fig. 10** Location of stationary symmetric vortex pairs over a wing-body combination of a flat-plate delta wing and an elliptic-cone body vs  $K$ ,  $\gamma = 0.7$ ,  $\tau = 1.5$ ,  $K_S = 0.0$ .

vortices are both initially unstable for small  $K_S$ . The windward (lower) vortex becomes stable when  $K_S$  is 0.016. Both vortices become stable when  $K_S$  is increased to 0.433. This means that sufficient sideslip can make the originally unstable symmetric vortex pair at zero sideslip to become stable but asymmetric.

**B. Flat-Plate Delta Wing and Elliptic-Cone Combinations**

Consider the case when the body-width-to-wing-span ratio  $\gamma = 0.7$  and the thickness ratio of the elliptic body  $\tau = 1.5$  under zero sideslip. Figure 10 shows the location of possible stationary symmetric vortex pairs vs  $K$  in the range from 1.0 to 8.0. The symmetric vortex pair first appears near the upper surface of the wing and moves upward and outboard as  $K$  is increased from 1. The vortex movement is extraordinarily large when  $K$  is increased from 4 to 5, and when  $K \geq 5.0$  the symmetric vortex pair is located higher than the uppermost point of the body. No stationary asymmetric vortex solutions are found for  $K \leq 4.66$ .

Figure 11 shows the eigenvalues of the symmetric vortex pair vs  $K$ . The vortex pair is stable when  $K < 4.4$  and unstable when  $K > 4.4$ . This transition happens right between  $K = 4$  and 5 when the symmetric vortex pair is moving abruptly away from the wing to over the body top.

To examine the effect of the body thickness ratio  $\tau$ , the preceding configuration with  $\gamma = 0.7$  is considered at a fixed  $K = 3.0$  and zero sideslip but varying  $\tau$ . Figure 12 shows the location of possible stationary symmetric and asymmetric vortex pairs vs  $\tau$ . The symmetric solution exists in the whole computed range of  $\tau$  from 0.0 to 1.5. Asymmetric vortex pair solutions are found only for  $0.4 < \tau < 1.5$ . The lower vortex of the asymmetric solution moves downward and outboard monotonically with increasing  $\tau$ . However, the upper vortex moves upward and outboard as  $\tau$  increases from 0.4 to 1.0 and then downward and inboard when  $\tau$  changes from 1.0 to 1.5. At  $\tau = 1.5$  the asymmetric vortex pair reduces to the symmetric solution.

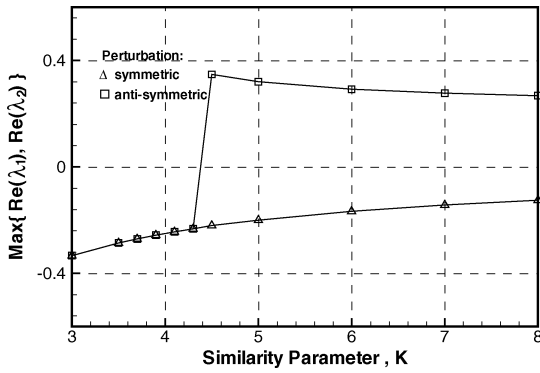


Fig. 11 Maximum real part of the eigenvalues for symmetric vortex pairs over a wing-body combination of a flat-plate delta wing and an elliptic-cone body vs  $K$ ,  $\gamma = 0.7$ ,  $\tau = 1.5$ ,  $K_S = 0.0$ .

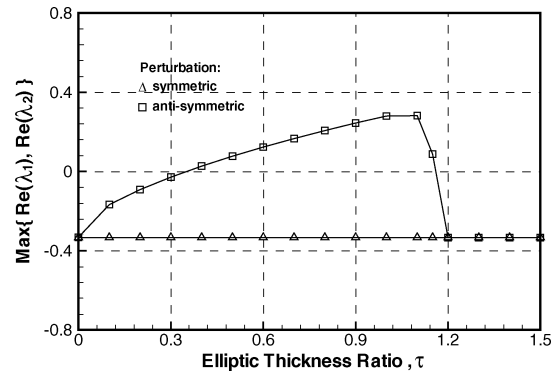


Fig. 13 Maximum real part of the eigenvalues for symmetric vortex pairs over a wing-body combination of a flat-plate delta wing and an elliptic-cone body vs  $\tau$ ,  $\gamma = 0.7$ ,  $K = 3.0$ ,  $K_S = 0.0$ .

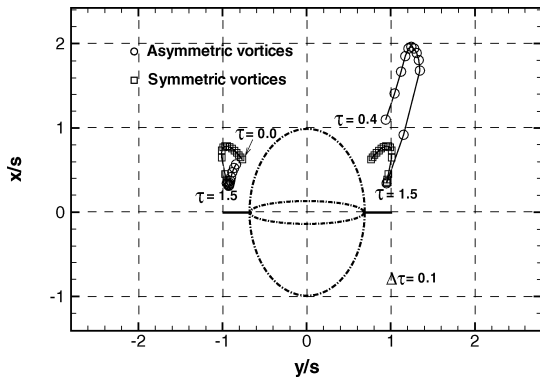


Fig. 12 Location of stationary symmetric and asymmetric vortex pairs over a wing-body combination of a flat-plate delta wing and an elliptic-cone body vs  $\tau$ ,  $\gamma = 0.7$ ,  $K = 3.0$ ,  $K_S = 0.0$ .

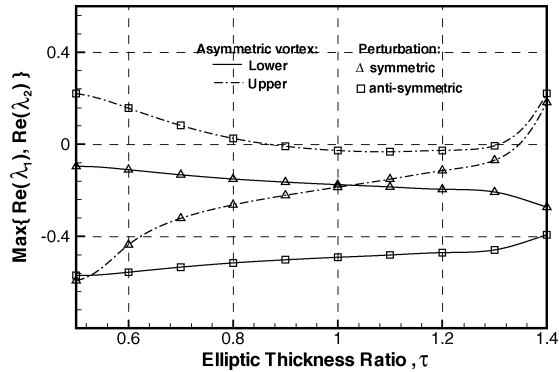


Fig. 14 Maximum real part of the eigenvalues for asymmetric vortex pairs over a wing-body combination of a flat-plate delta wing and an elliptic-cone body vs  $\tau$ ,  $\gamma = 0.7$ ,  $K = 3.0$ ,  $K_S = 0.0$ .

Figures 13 and 14 show the eigenvalues vs  $\tau$  for the symmetric and asymmetric vortex pairs, respectively. The symmetric vortex pair is stable for  $\tau < 0.35$  (thin centerbody) and  $\tau > 1.16$  (thick centerbody) and unstable otherwise. The asymmetric vortex pair is stable only for  $0.86 < \tau < 1.31$ . For very small  $\tau$ , the centerbody is rather flat, and thus the wing-body combination approaches that of a flat-plate wing, for which we know that no asymmetric solution exists and the symmetric solution is stable.<sup>15</sup> For very large thickness ratios, the centerbody becomes very tall and has the effect of reducing the interaction between the two vortices and thus enhances the stability of a symmetric vortex pair. It is in the midrange of  $\tau$  that the flow tends to encourage the appearance of an asymmetric vortex pair.

Shanks<sup>25</sup> performed wind-tunnel tests of highly swept delta wings with semiapex angles of 6 to 20 deg at high angles of attack up to 40 deg. His measurements showed the appearance of significant rolling moments at angles of attack above 24 deg and zero sideslip for models whose semiapex angles are less than 12 deg. Shanks's experiment led to the belief that the vortex flow over a low-aspect-ratio delta wing with sharp leading edges, like the flow over slender pointed bodies of revolution, would become asymmetric at high angles of attack and zero sideslip before vortex breakdown occurs over the wing (for example, see Ref. 29). Later, Stahl et al.<sup>13</sup> performed water-tunnel and wind-tunnel experiments and concluded based on their force measurements and flow visualization that the vortex flow over slender delta wings with sharp leading edges remained symmetric at all angles of attack until vortex breakdown occurred on the wing. That conclusion seemingly contradicted the observations by Shanks. Ericsson,<sup>30</sup> however, noticed that Shanks's wing model differed from that by Stahl et al. in that Shanks's model contained a low center-spline or "fuselage bump" on the leeside of the wing. Ericsson claimed that the vortex asymmetry observed in Shanks's experiment was not caused by hydrodynamic instability but rather likely caused by asymmetric reattachment in the presence of the center-spline.

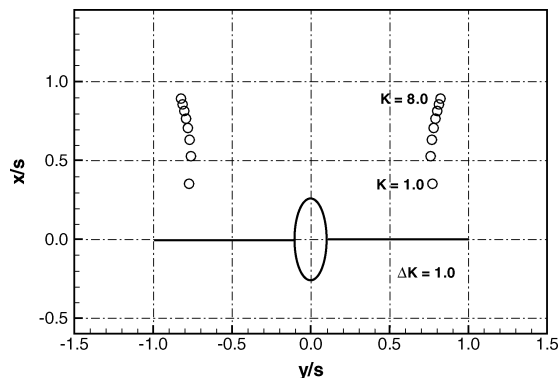


Fig. 15 Location of stationary symmetric vortex pairs over a wing-body combination of a flat-plate delta wing and an elliptic-cone body vs  $K$ ,  $\gamma = 0.1$ ,  $\tau = 2.5$ ,  $K_S = 0.0$ .

This controversy led to the previous study by the authors<sup>14</sup> of the vortex stability over a delta wing with a triangular flat-plate dorsal fin. The stability analysis reveals that vortices over a flat-plate delta wing at zero sideslip are conical, symmetric, and stable for all angles of attack, but adding a low dorsal fin to the wing would destabilize the vortices. The flow would recover symmetry only when the fin height is increased to a critical level. This finding points out that the vortex asymmetry observed in Shanks's experiment was indeed caused by the destabilizing effect of the short fuselage bump. In addition, this loss of symmetry is caused by the flow instability as a result of the inviscid hydrodynamic interactions between the two vortices.

However, the round fuselage bump in Shanks's experiment was simulated by a zero-thickness flat-plate fin in the analysis of Ref. 14. A round fuselage bump allows an extra degree of freedom in the vortex reattachment point. In view of this, we consider the combination of a narrow but tall elliptic center body and flat-plate delta-wing

combination with  $\tau = 2.5$  and  $\gamma = 0.1$ . The small  $\gamma$  and large  $\tau$  values are used here so that the centerbody much resembles the fuselage bump in Shanks's experiment. Figure 15 shows the location of possible stationary symmetric vortex pairs vs  $K$ . The symmetric vortex pair moves upward and outboard as  $K$  increases. Figure 16 shows the eigenvalues of the vortex pair vs  $K$ . The vortex pair loses its stability when  $K$  exceeds about 3.3, which is not too far from the observed critical value of  $K \approx 4.0$  in Shanks's experiment corresponding to an angle of attack of 24 deg. The fuselage bump in Shanks's experiment was only on the upper surface of the wing, whereas our analytical model adds such a bump also on the lower surface, which might explain the fact that the vortices lose stability at a smaller  $K$  value compared to that of the experiment. This further affirms the conclusion that the loss of symmetry in Shanks's experiment is caused by a hydrodynamic instability of the vortices brought about by the displacement effect of the small fuselage bump. The position of reattachment of the flow on the wing is not a factor.

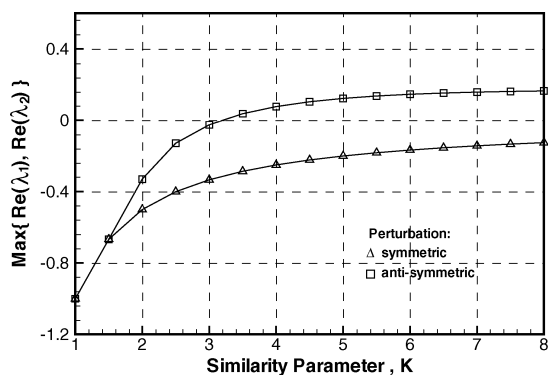


Fig. 16 Maximum real part of the eigenvalues for symmetric vortex pairs over a wing-body combination of a flat-plate delta wing and an elliptic-cone body vs  $K$ ,  $\gamma = 0.1$ ,  $\tau = 2.5$ ,  $K_S = 0.0$ .

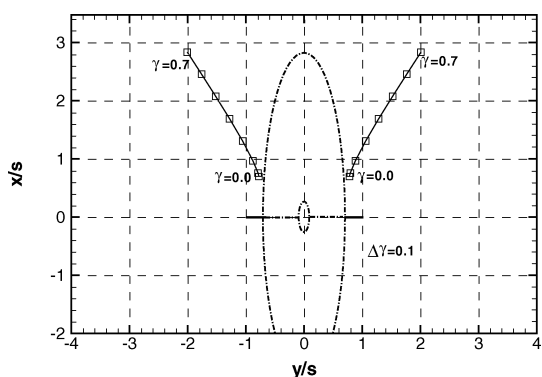


Fig. 17 Location of stationary symmetric vortex pairs over a wing-body combination of a flat-plate delta wing and an elliptic-cone body vs  $\gamma$ ,  $\tau = 4.0$ ,  $K = 4.0$ ,  $K_S = 0.0$ .

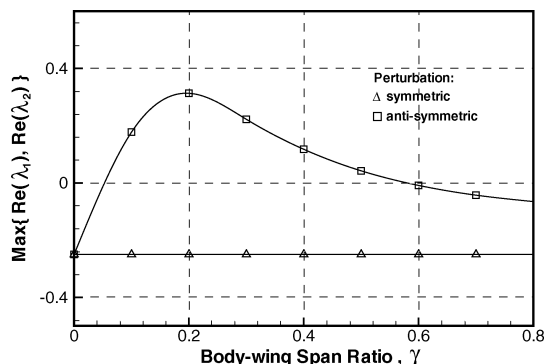


Fig. 18 Maximum real part of the eigenvalues for symmetric vortex pairs over a wing-body combination of a flat-plate delta wing and an elliptic-cone body vs  $\gamma$ ,  $\tau = 4.0$ ,  $K = 4.0$ ,  $K_S = 0.0$ .

Finally, for completeness, we consider a rather thick centerbody ( $\tau = 4.0$ ) with varying relative body width to the delta-wing span, that is,  $\gamma$  at a fixed  $K = 4.0$ . Figure 17 shows the location of possible stationary symmetric vortex pairs vs  $\gamma$  ranging from 0.0 to 0.7. The symmetric vortex pair moves continuously upward and outboard as  $\gamma$  is increased. Stationary asymmetric vortex solutions can be found but are not shown in the figure for this case when  $\gamma$  is very large. Figure 18 shows the eigenvalues of the symmetric vortex system vs  $\gamma$ . The vortex pair is stable except for  $\gamma$  in the range between 0.05 and 0.57. As  $\gamma$  increases from 0, the initially stable symmetric vortex pair first becomes unstable because of the existence of the fuselage-bump-like object on the wing, and then changes back to be stable because the greatly increased height of the elliptic cone reduces the interaction of the vortex pair.

#### IV. Conclusions

The stability theory developed in Ref. 14 for vortex pairs over conical slender bodies in an inviscid, incompressible flow at high angles of attack is applied to study the stability of symmetric and asymmetric vortex pairs over flat-plate delta wing and circular cone or elliptic cone combinations. A wide range of parametric studies has been performed. Results are compared with available experimental data. They help gain insight of the physics of the flow. The analytical formulation can also be used to develop reduced-order models for the development of active flow control. Some of the findings of the present study are summarized next.

By adding a delta wing to the circular-cone body, an originally unstable vortex pair over the circular cone becomes stable when the wing span is large enough relative to the body diameter. The present analytical results confirm the well-known effect of nose strakes in suppressing flow asymmetry about pointed slender body at high angles of attack. The effect of a pair of horizontal strakes is to force the separation line to the leading edge of the strake so as to widen the distance between the two vortices and thus reduce their mutual interaction.

When  $K$  is sufficiently large or the body-width-to-wing-span ratio  $\gamma$  is large enough for a circular-cone and flat-plate delta-wing combination, there exists stationary asymmetric vortex pairs in addition to stationary symmetric vortex pairs. An initially stable symmetric vortex pair can transit into a stable asymmetric pair as  $K$  increases for a given configuration. In addition, for a given  $K$  an unstable stationary symmetric vortex pair at zero sideslip can change to a stable asymmetric vortex pair when the sideslip similarity parameter  $K_S$  is large enough. In other words, sideslip can stabilize an originally unstable symmetric vortex pair at no sideslip.

Both the present analysis using a tall elliptic centerbody to represent the fuselage bump in Shanks's delta wing model and that of Ref. 14 using a zero-thickness flat-plate fin affirm the finding that the flow asymmetry observed by Shanks<sup>25</sup> over his delta wing is of the origin of hydrodynamic instability caused by the destabilizing effect of the short leeward-side bump on his test model. The position of reattachment of the flow on the wing is not important. Stability can be restored by using a sufficiently high fin with either sharp or rounded edge because the height of the vertical fin reduces the hydrodynamic interaction between the two vortices.

#### References

- Hunt, B. L., "Asymmetric Vortex Forces and Wakes on Slender Bodies," AIAA Paper 82-1336, Aug. 1982.
- Ericsson, L., and Reding, J., "Asymmetric Flow Separation and Vortex Shedding on Bodies of Revolution," *Tactical Missile Aerodynamics: General Topics*, Vol. 141, Progress in Astronautics and Aeronautics, edited by M. Hemsh, AIAA, New York, 1992, pp. 391-452.
- Champigny, P., "Side Forces at High Angles of Attack. Why, When, How?" *La Recherche Aeronautique*, No. 4, 1994, pp. 269-282.
- Lamont, P. J., "Pressures Around an Inclined Ogive Cylinder with Laminar, Transitional, or Turbulent Separation," *AIAA Journal*, Vol. 20, No. 11, 1982, pp. 1492-1499.
- Zilliacci, G. G., Degani, D., and Tobak, M., "Asymmetric Vortices on a Slender Body of Revolution," *AIAA Journal*, Vol. 29, No. 5, 1991, pp. 667-675.

- <sup>6</sup>Degani, D., "Effect of Geometrical Disturbance on Vortex Asymmetry," *AIAA Journal*, Vol. 29, No. 4, 1991, pp. 560–566.
- <sup>7</sup>Degani, D., "Instabilities of Flows over Bodies at Large Incidence," *AIAA Journal*, Vol. 30, No. 1, 1992, pp. 94–100.
- <sup>8</sup>Hartwich, P. M., Hall, R. M., and Hemsch, M. J., "Navier–Stokes Computations of Vortex Asymmetries Controlled by Small Surface Imperfections," *Journal of Spacecraft and Rockets*, Vol. 28, No. 2, 1991, pp. 258–264.
- <sup>9</sup>Dyer, D. E., Fiddes, S. P., and Smith, J. H. B., "Asymmetric Vortex Formation from Cones at Incidence—A Simple Inviscid Model," *Aeronautical Quarterly*, Vol. 33, Pt. 4, Nov. 1982, pp. 293–312.
- <sup>10</sup>Chin, S., Lan, C. E., and Gainer, T. G., "Calculation of Asymmetric Vortex Separation on Cones and Tangent Ogives Based on a Discrete Vortex Model," *AIAA Journal*, Vol. 27, No. 12, 1989, pp. 1824–1826.
- <sup>11</sup>Pidd, M., and Smith, J. H. B., "Asymmetric Vortex Flow over Circular Cones," *Vortex Flow Aerodynamics*, AGARD CP-494, 1991, pp. 18–11.
- <sup>12</sup>Huang, M. K., and Chow, C. Y., "Stability of Leading-Edge Vortex Pair on a Slender Delta Wing," *AIAA Journal*, Vol. 34, No. 6, 1996, pp. 1182–1187.
- <sup>13</sup>Stahl, W., Mahmood, M., and Asghar, A., "Experimental Investigations of the Vortex Flow on Delta Wings at High Incidence," *AIAA Journal*, Vol. 30, No. 4, 1992, pp. 1027–1032.
- <sup>14</sup>Cai, J., Liu, F., and Luo, S., "Stability of Symmetric Vortices in Two-Dimensions and over Three-Dimensional Slender Conical Bodies," *Journal of Fluid Mechanics*, Vol. 480, April 2003, pp. 65–94.
- <sup>15</sup>Cai, J., Luo, S., and Liu, F., "Stability of Symmetric and Asymmetric Vortex Pairs over Slender Conical Wings and Bodies," *Physics of Fluids*, Vol. 16, No. 2, 2004, pp. 424–432.
- <sup>16</sup>Coe, P., Chambers, J., and Letko, W., "Asymmetric Lateral-Directional Characteristics of Pointed Bodies of Revolution at High Angle of Attack," NASA TN D-7095, Nov. 1972.
- <sup>17</sup>Erickson, G. E., and Lorincz, D. J., "Water Tunnel and Wind Tunnel Studies of Asymmetric Load Alleviation on a Fighter Aircraft at High Angles of Attack," AIAA Paper 80-1618, Aug. 1980.
- <sup>18</sup>Nelson, R., and Malcolm, G., "Visualization of High-Angle-of-Attack Flow Phenomena," *Tactical Missile Aerodynamics: General Topics*, Vol. 141, Progress in Astronautics and Aeronautics, edited by M. Hemsh, AIAA, New York, 1992, pp. 195–250.
- <sup>19</sup>Malcolm, G., "Forebody Vortex Control," *Progress in Aerospace Sciences*, Vol. 28, No. 3, 1991, pp. 171–234.
- <sup>20</sup>Murri, D., and Rao, D., "Exploratory Studies of Actuated Forebody Strakes for Yaw Control at High Angles of Attack," AIAA Paper 87-2557, Sept. 1987.
- <sup>21</sup>Protas, B., "Linear Feedback Stabilization of Laminar Vortex Shedding Based on a Conical Wings and Bodies," *Physics of Fluids*, Vol. 16, No. 12, 2004, pp. 4473–4487.
- <sup>22</sup>Sychev, V., "Three-Dimensional Hypersonic Gas Flow past Slender Bodies at High Angle of Attack," *Journal of Math. and Mech. (USSR)*, Vol. 24, Feb. 1960, pp. 296–306.
- <sup>23</sup>Rossow, V. J., "Lift Enhancement by an Externally Trapped Vortex," *Journal of Aircraft*, Vol. 15, No. 9, 1978, pp. 618–625.
- <sup>24</sup>Keener, E. R., Chapman, G. T., Chohen, L., and Talaghani, J., "Side Forces on Forebodies at High Angles of Attack and Mach Numbers from 0.1 to 0.7," NASA TM X-3438, Feb. 1977.
- <sup>25</sup>Shanks, R., "Low-Subsonic Measurements of Static and Dynamic Stability Derivatives of Six Flat-Plate Wing Having Leading-Edge Sweep Angles of 70° to 84°," NASA TN D-1822, July 1963.
- <sup>26</sup>Meng, X., Qiao, Z., Gao, C., Luo, S., and Liu, F., "Visualization of Vortex Flow over Delta Wing with Dorsal Fin," AIAA Paper 2005-1058, Jan. 2005.
- <sup>27</sup>Asghar, A., Stahl, W., and Mahmood, M., "Suppression of Vortex Asymmetry and Side Force on a Circular Cone," *AIAA Journal*, Vol. 32, No. 10, 1994, pp. 2117–2120.
- <sup>28</sup>Ng, T., "Effect of a Single Strake on the Fore Body Vortex Asymmetry," *Journal of Aircraft*, Vol. 27, No. 9, 1990, pp. 844–846.
- <sup>29</sup>Keener, E., and Chapman, G., "Similarity in Vortex Asymmetries over Slender Bodies and Wings," *AIAA Journal*, Vol. 15, No. 9, 1977, pp. 1370–1372.
- <sup>30</sup>Ericsson, L., "Sources of High Alpha Vortex Asymmetry at Zero Sideslip," *Journal of Aircraft*, Vol. 29, No. 6, 1992, pp. 1086–1090.

A. Plotkin  
Associate Editor